OPEN

The ISME Journal (2016) 10, 897–910

www.nature.com/ismej

ORIGINAL ARTICLE

# An intracellular replication niche for *Vibrio cholerae* in the amoeba *Acanthamoeba castellanii*

Charles Van der Henst[1], Tiziana Scrignari[1], Catherine Maclachlan[2] and Melanie Blokesch[1]
[1]*Laboratory of Molecular Microbiology, Global Health Institute, School of Life Sciences, Station 19, EPFL-SV-UPBLO, Ecole Polytechnique Fédérale de Lausanne (EPFL), Lausanne, Switzerland and*
[2]*Bioelectron Microscopy Core Facility (BioEM), School of Life Sciences, Station 19, EPFL-SV-PTBIOEM, Ecole Polytechnique Fédérale de Lausanne (EPFL), Lausanne, Switzerland*

***Vibrio cholerae*** **is a human pathogen and the causative agent of cholera. The persistence of this bacterium in aquatic environments is a key epidemiological concern, as cholera is transmitted through contaminated water. Predatory protists, such as amoebae, are major regulators of bacterial populations in such environments. Therefore, we investigated the interaction between** ***V. cholerae*** **and the amoeba** ***Acanthamoeba castellanii*** **at the single-cell level. We observed that** ***V. cholerae*** **can resist intracellular killing. The non-digested bacteria were either released or, alternatively, established a replication niche within the contractile vacuole of** ***A. castellanii. V. cholerae*** **was maintained within this compartment even upon encystment. The pathogen ultimately returned to its aquatic habitat through lysis of** ***A. castellanii*****, a process that was dependent on the production of extracellular polysaccharide by the pathogen. This study reinforces the concept that** ***V. cholerae*** **is a facultative intracellular bacterium and describes a new host–pathogen interaction.**
*The ISME Journal* (2016) **10,** 897–910; doi:10.1038/ismej.2015.165; published online 22 September 2015

## Introduction

Cholera, a severe diarrheal disease caused by the pathogenic bacterium *Vibrio cholerae*, remains a serious health threat. Because *V. cholerae* is an aquatic bacterium and is primarily encountered in coastal waters, estuaries, ponds and rivers, its re-emergence is thought to be climate-related (Colwell, 1996; Morens *et al.*, 2004). In its environmental reservoir, *V. cholerae* is found not only in a free-living state but also in association with phytoplankton, zooplankton and potentially also with additional environmental hosts.

Until recently, a lot of the research on *V. cholerae* has focused directly on the clinical aspects. However, the insidious and complex nature of the pathogen still requires more investigations covering the environmental lifestyle of *V. cholerae*. In an environmental context, predation by protists and particularly amoebae represents a major selective pressure that shapes bacterial populations (Matz and Kjelleberg, 2005; Pernthaler, 2005; Snelling *et al.*, 2006). Moreover, amoebae are widely used as non-mammalian model organisms in research of host–microbe interactions. Previous studies have addressed the killing behavior of few specific *V. cholerae* isolates towards the social amoeba *Dictyostelium discoideum* (Pukatzki *et al.*, 2006). However, as *D. discoideum* is primarily a soil-living amoeba, recurrent encounters with *V. cholerae* are unlikely. The free-living amoeba *Acanthamoeba castellanii*, however, is frequently found in aquatic environments (Martinez and Visvesvara, 1997; Khan, 2006, 2015). These amoebae prey on bacteria and have been described as a reservoir of pathogenic bacteria (Fouque *et al.*, 2012). *A. castellanii* is characterized by a biphasic life cycle; the 'trophozoite' form is metabolically active and feeding, and the 'cyst' form is stress-induced, dormant and resistant to various environmental hazards (Khan, 2006). Successive steps of encystment occur in the progression from the trophozoite to the mature cyst, including global cell rounding and increased cell-wall synthesis (Bowers and Korn, 1968; Fouque *et al.*, 2012; Chavez-Munguia *et al.*, 2013). As a result, cysts harbor a thickened cell wall, which enhances their resistance to disinfection treatments.

Though an impact of predatory flagellates on *V. cholerae* populations has been established (Matz *et al.*, 2005), much less is known about the interaction of *V. cholerae* with free-living amoebae and the molecular mechanisms underlying such an interaction. Notably, *V. cholerae* and *A. castellanii* were detected in the same environmental habitats (Shanan *et al.*, 2011) and a study by Thom *et al.*

Correspondence: M Blokesch, Laboratory of Molecular Microbiology, Global Health Institute, School of Life Sciences, Station 19, EPFL-SV-UPBLO, Ecole Polytechnique Fédérale de Lausanne (EPFL), CH-1015 Lausanne, Switzerland.
E-mail: melanie.blokesch@epfl.ch
Received 24 April 2015; revised 2 August 2015; accepted 10 August 2015; published online 22 September 2015

(1992) showed that *V. cholerae* survived better in the presence of the amoebae *Acanthamoeba polyphaga* and *Naegleria gruberi* compared with that in their absence. Follow-up work by the Sandström group confirmed the increased survival of *V. cholerae* in the presence of *Acanthamoebae* (Abd *et al.*, 2005, 2007; Sandström *et al.*, 2010; Shanan *et al.*, 2011). Notably, these and other studies (Sun *et al.*, 2013) focused primarily on population measurements including the enumeration of colony-forming units, whereas limited information was provided at the single-cell level.

This study aimed at deciphering the interaction of *V. cholerae* and amoeba using imaging-based approaches. We hypothesized that the pathogen could grow intracellulary within an environmental non-human host. The rationale for these speculations was based on two observations: (i) Nielsen *et al.* (2010) provided evidence of intracellular growth of *V. cholerae* within extruded epithelial cells, a phenotype that was observed in a rabbit ileal loop model of cholera; and (ii) the association of the pathogen with so-called 'ghost cells' was recently reported based on the evaluation of stool samples from cholera patients (Nelson *et al.*, 2007). The authors defined such ghost cells as DAPI (4′,6-diamidino-2-phenylindole) stain-negative cells with a size range of 20–80 μm, which were most likely derived from the mucosal epithelium (Nelson *et al.*, 2007).

Considering the primary niche of this pathogen, it is tempting to speculate that aquatic amoebae could serve as environmental hosts for *V. cholerae* and might select for pathogenic traits, a phenomenon that has been suggested for other human pathogens such as *Legionella pneumophila* (Solomon and Isberg, 2000; Swanson and Hammer, 2000; Greub and Raoult, 2004; Hoffmann *et al.*, 2014). In this study, we hypothesized that the putative intracellular occurrence of *V. cholerae* (in rabbits and humans; Nelson *et al.*, 2007; Nielsen *et al.*, 2010) might represent an adaptive trait of *V. cholerae* acquired in aquatic reservoirs. We therefore investigated the interaction of *V. cholerae* and *A. castellanii* at the single-cell level. We show that *V. cholerae* bacteria can (i) resist intracellular killing by *A. castellanii*; (ii) be released from trophozoites by exocytosis; (iii) establish an intracellular proliferation niche; (iv) maintain their niche upon amoebal encystment; and (v) promote the lysis of *A. castellanii* cysts. Moreover, we demonstrate that a functional quorum sensing (QS) circuit and the *Vibrio* polysaccharide (VPS) are of importance for this host–pathogen interaction. Our data reinforce the concept that *V. cholerae* is a facultative intracellular pathogen and strongly suggest that this intracellular lifestyle enhances environmental survival and proliferation.

## Materials and methods

*Amoebal and bacterial strains and plasmids*

The *Vibrio cholerae* strains used in this study are derived from O1 El Tor strain A1552 (Yildiz and Schoolnik, 1998) and are listed in Table 1 (together with the plasmids). To delete the *vpsA* (VC0917) or *hapR* (VC0583) genes from the parental wild-type (WT) strain (A1552), a gene disruption method based on natural transformation and FLP recombination was used (TransFLP method; De Souza Silva and Blokesch, 2010; Marvig and Blokesch, 2010; Blokesch, 2012a; Borgeaud and Blokesch, 2013). The site-directed stable insertion of the mini-Tn7-derived transposons (mTn7-GFP (green fluorescent protein), mTn7-dsRed and mTn7-rrnBP1-gfp(ASV))

**Table 1** *V. cholerae* strains and plasmids used in this study

| | *Genotype/description*[a] | *Reference* |
|---|---|---|
| *Strains* | | |
| A1552 (WT) | Wild-type, O1 El Tor Inaba, $Rif^R$ | Yildiz and Schoolnik (1998) |
| A1552-GFP | A1552 with mTn7-*gfp;* $Rif^R$, $Gent^R$ | Blokesch (2012b) |
| A1552-dsRed | A1552 with mTn7-*dsRed.T3[DNT]*; $Rif^R$, $Gent^R$ | Borgeaud *et al.* (2015) |
| A1552-Tn*rrnBP1-gfp(ASV)* | A1552 with mTn7-*rrnBP1-gfp(ASV)*; $Rif^R$, $Gent^R$; growth reporter strain | This study |
| ΔhapR | A1552 deleted for *hapR* (TransFLP); $Rif^R$ | Borgeaud *et al.* (2015) |
| ΔhapR-GFP | ΔhapR with mTn7-*gfp*; $Rif^R$, $Gent^R$ | This study |
| ΔhapR-dsRed | ΔhapR with mTn7-*dsRed.T3[DNT]*; $Rif^R$, $Gent^R$ | This study |
| ΔhapRΔvpsA | A1552 deleted for *hapR* and *vpsA* (TransFLP); $Rif^R$ | This study |
| ΔhapRΔvpsA-GFP | ΔhapRΔvpsA with mTn7-*gfp*; $Rif^R$, $Gent^R$ | This study |
| ΔhapRΔvpsA-dsRed | ΔhapRΔvpsA with mTn7-*dsRed.T3[DNT]*; $Rif^R$, $Gent^R$ | This study |
| ΔvpsA | A1552 deleted for *vpsA* (TransFLP); $Rif^R$ | This study |
| ΔvpsA-GFP | ΔvpsA with mTn7-*gfp*; $Rif^R$, $Gent^R$ | This study |
| *Plasmids* | | |
| pUX-BF13 | *ori*R6K, helper plasmid with Tn7 transposition function; $Amp^R$ | Bao *et al.* (1991) |
| pGP704::Tn7-GFP | pGP704 with mini-Tn7 harboring a constitutively expressed *gfp* cassette; $Amp^R$ | Müller *et al.* (2007) |
| pGP704-mTn7-dsRed | pGP704 with mini-Tn7 carrying *dsRed.T3[DNT]*; $Amp^R$ | Borgeaud *et al.* (2015) |
| pGP704Sac28-mTn7-rrnBP1-gfp(ASV) | pGP704 with mini-Tn7 carrying growth reporter *rrnBP1-gfp(ASV)*; $Amp^R$ | This study |

[a]TransFLP method according to De Souza Silva and Blokesch (2010) and Blokesch (2012a).

into the chromosome of the indicated strains was accomplished through triparental mating (Bao *et al.*, 1991). *Escherichia coli* strain S17-1λpir/pGP704-mTn7-dsRed served as a non-pathogenic control. *Acanthamoeba castellanii* Neff strain, genotype T4 (American Type Culture Collection 30010 (ATCC30010)) was used in all amoebal experiments.

*Media and growth conditions*
Uninfected amoebae were grown in peptone yeast glucose medium (ATCC medium 712). Bacterial cultures were grown in LB medium at 30 °C under shaking conditions. Defined artificial seawater medium at a 0.5-fold concentration and buffered with 50 mM HEPES (Meibom *et al.*, 2005) served as the infection medium. Antibiotics were supplemented when required at the following concentrations: gentamicin, 50 μg ml$^{-1}$; ampicillin, 100 μg ml$^{-1}$; streptomycin, 100 μg ml$^{-1}$.

*Amoebal infections*
For the evaluation of bacterial uptake by the amoebae, an infection protocol was implemented for confocal microscopy imaging, in which adherent *A. castellanii* trophozoites ($1 \times 10^5$ cells per ml) were infected with the bacteria (multiplicity of infection of 1000) in 35 mm μ-Dish devices (IBIDI, Martinsried, Germany). The incubation occurred statically at 24 °C. Single-cell quantification (contractile vacuole (CV) colonization in trophozoites, CV colonization in cysts, cytosol colonization in cysts and colonized lysed cysts) was carried out at 20 h after post primary contact (p.p.c.). The evaluation was based on at least 1200 counted amoebae per experiment and the data show averages from three independent biological replicates.

For the enumeration of surviving bacteria, the amoebal and bacterial cells were detached from the IBIDI device using a cell scraper. The homogenized amoebae were lysed by three cycles (30 s on, 30 s off) of bead beating (glass beads of 0.75–1 mm diameter; Retsch GmbH, Haan, Germany) using a Precellys 24 homogenizer (Bertin Technologies, Montigny-le-Bretonneux, France) at a speed of 5000 r.p.m. This method allowed the lysis of both trophozoites and cysts of *A. castellanii* as visually inspected. Recovered bacteria were serial diluted, spotted onto agar plates and enumerated the following day (given as colony-forming units (CFUs) per ml).

*Confocal laser scanning microscopy*
Confocal laser scanning microscopy images were obtained using an inverted Zeiss LSM 700 confocal microscope (Zeiss, Feldbach, Switzerland) equipped with four laser lines, two confocal channels and a highly sensitive photomultiplier for the detection of transmission signals. For time-lapse imaging, pictures were taken every 30 s in one plane.

To follow the phago-/endosomal pathway of the amoebae, the infection medium was supplemented with Alexa Fluor 647-labeled dextran (size: 10 000-MW; Molecular Probes and purchased via Life Technologies, Zug, Switzerland) at a final concentration of 100 μg ml$^{-1}$ and fluorescence was monitored in the far-red region (excitation and emission wavelengths are 650 and 668, respectively). One-micrometer Fluoresbrite Yellow Green (YG) microspheres (Polysciences Inc., Eppelheim, Germany) were used at a concentration of ~$10^7$ particles per ml.

*Fluorescence recovery after photobleaching*
Fluorescence recovery after photobleaching was used to test for bacterial protein synthesis and therefore bacterial viability within the CV of infected amoebae. *V. cholerae* were subjected to 20 iterations of bleaching throughout the full Z-direction of the amoeba using the 488 nm laser line at 100% power. Epifluorescence microscopy images were taken to confirm the complete bleaching of the CV. Fluorescence recovery was monitored after 30, 60 and 90 min using the confocal laser scanning option with the same scanning settings. Quantification of the fluorescent signal was performed using ImageJ (National Institute of Mental Health, Bethesda, MD, USA).

*Electron microscopy*
Infected amoebae were initially fixed in a solution of 1% acrolein and 1% glutaraldehyde in 0.1M cacodylate buffer using a microwave (Pelco BioWave; Ted Pella, Redding, CA, USA; 30 s at 300, 350 and 400 W) to ensure rapid preservation. Samples were then left for 60 min in the same fixative before being pelleted by gentle centrifugation. The supernatant was replaced by 4% low melting-point agarose (w v$^{-1}$) in 0.1 M cacodylate and the pellet was resuspended. After cooling on ice, the agarose was cut into small cubes (~0.5 mm each side length) with a razor blade. These cubes were again fixed using the same fixative as above, washed in 0.1 M cacodylate buffer and then stained using 1% osmium (w v$^{-1}$) in 0.1 M cacodylate buffer followed by 1% uranyl acetate (w v$^{-1}$) in 0.1 M cacodylate, for 40 min each. The samples were dehydrated in increasing concentrations of ethanol, transferred to propylene oxide and infiltrated for 24 h with epon resin. The samples were embedded between two glass slides and placed in a 65 °C oven for 24 h. The embedded samples were visualized using a dissecting microscope and blocks were prepared from these regions. Fifty nanometer-thick sections were cut using an ultramicrotome (Leica EM UC7; Leica Microsystems AG, Heerbrugg, Switzerland) and collected on formvar-coated slot grids. Finally, the samples were stained with 1% uranyl acetate (w v$^{-1}$) followed by 3% lead citrate (w v$^{-1}$). Images were collected in a transmission electron microscope (Tecnai Spirit; FEI Company,

Eindhoven, Netherlands) at 80 KV using a digital camera (Eagle; FEI Company).

*Statistical analysis*
Two-way analysis of variance with Tukey's post-test was performed using GraphPad Prism version 6.00 for Mac (GraphPad Software, San Diego, CA, USA).

## Results

*Release of viable V. cholerae from the amoeba A. castellanii*
Even though outside of blooms (Gilbert *et al*., 2012) *Vibrios* represent on average only a few percent of total bacteria (with $10^3$–$10^4$ bacteria per ml), they can contribute significantly to the biomass in aquatic environments (Yooseph *et al*., 2010). Such balanced biomass is based on rapid growth combined with high predation (Takemura *et al*., 2014). As predatory free-living amoebae and *V. cholerae* occur in the same ecological niche (Thom *et al*., 1992), it is plausible that the two organisms have coevolved based on frequent encounters. We therefore aimed at better understanding the interaction between *A. castellanii* and *V. cholerae* at the single-cell level. GFP-producing *V. cholerae* bacteria were monitored by time-lapse imaging, allowing observation of active internalization of the bacteria by amoebae (Figure 1a and Supplementary Movie S1). Such bacterial uptake resulted in small, bacteria-filled vacuoles, which eventually fused to form larger compartments. Based on the retained morphology observed by electron microscopy (Figure 1b) and the release of non-digested bacteria (see below), we concluded that at least a fraction of the internalized bacteria were not digested within these vacuoles. In contrast to previous studies (Abd *et al*., 2005, 2007), we did not observe *V. cholerae* cells within the cytosol of the trophozoites even though mitochondria were readily detectable (see Discussion). These data suggest that undigested *V. cholerae* are present within intracellular vacuoles of *A. castellanii* after phagocytosis.

To identify the compartment containing intracellular *V. cholerae*, we followed the course of the phago-/endosomal pathway by feeding amoebae undigestible fluorescently labeled high-molecular-weight dextran, and tracked its localization (Aubry *et al*., 1993). Similar to other cellular waste including digested bacteria, the accumulated dextran is ultimately released into the environment by exocytosis. At early time points (0–5 h p.p.c.), phagocytosed bacteria colocalized with the dextran, indicating that intracellular *V. cholerae* reside within food vacuoles (Figure 1c and quantified in Supplementary Figure S1). In addition, live-cell imaging provided evidence that such pathogen-containing compartments fused to form larger vacuoles, which the amoeba ultimately excreted by exocytosis, thereby releasing live bacteria back into the environment (Figure 2 and Supplementary Movie S2). Such release of undigested bacteria was not observed in the control experiments using non-pathogenic *E. coli* (Supplementary Figure S2B). We therefore conclude that, upon phagocytosis, a portion of the *V. cholerae* population resisted intracellular killing and returned to the environment.

*V. cholerae escapes the endosomal pathway through the water discharge system of A. castellanii*
After we had established the intracellular survival phenotype, we were curious to determine whether all ingested *V. cholerae* follow the same fate. Interestingly, quantification of the images showed that even though the vast majority of *A. castellanii* contained internalized *V. cholerae* within the phagosomal pathway, a small but consistently observed fraction of the amoebal population contained fluorescently labeled bacteria that did not colocalize with the fluorescent dextran (Figure 3a and quantified in Supplementary Figure S1). Instead, we witnessed the presence of *V. cholerae* accumulated inside the CV of *A. castellanii* (Figure 3a). The CV is a highly dynamic organelle involved in osmoregulation (Doberstein *et al*., 1993), which is readily visible in transmission-light images. It regulates osmotic pressure by collecting cytosolic water and actively discharging excess water by means of contraction (Allen 2000; Khan 2015). Upon closer inspection, we observed that colonization of the CV was nearly coincident with fusion of small food vacuoles (e.g., ~4 h p.p.c.). In accordance with this observation, we were able to image the entry of *V. cholerae* into the CV upon vacuolar fusion (Figure 3b and Supplementary Movie S3). Notably, we never observed colonization of the CV by *E. coli* (quantified in Supplementary Figure S1), suggesting that *V. cholerae* promotes these fusion events in an unknown (direct or indirect) manner. To confirm this, we first fed *A. castellanii* indigestible fluorescent microspheres. Upon phagocytosis, such beads were excluded from the CV and instead colocalized with the dextran, indicating passage through the regular phago-/endosomal pathway (Supplementary Figure S1B and quantified in Supplementary Table S1). However, upon coinoculation with *V. cholerae*, such beads became readily detectable within the CV (Figure 3c and quantified in Supplementary Table S1). Again, the same phenomenon was never observed when *E. coli* was used in place of *V. cholerae* (Supplementary Table S1). These data are indicative of a *V. cholerae*-promoted CV colonization process.

*CV-infected amoebae maintain the pathogen upon encystment followed by CV destruction and cyst lysis*
We followed the fate of the CV-infected *A. castellanii* over time (Supplementary Movie S4–S6). Under unfavorable conditions, the metabolically active amoebal trophozoites undergo a differentiation

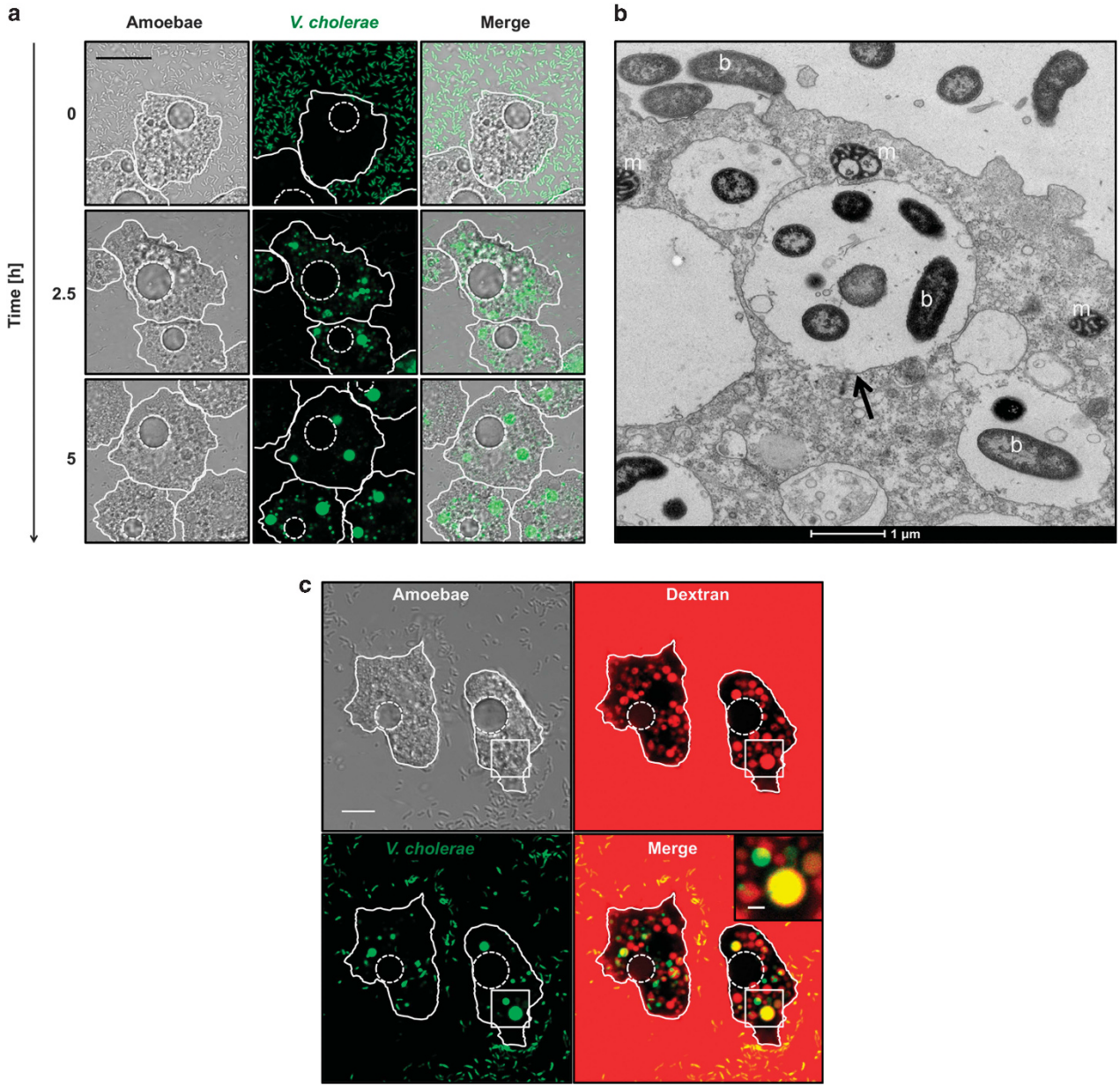


**Figure 1** Uptake of *V. cholerae* by *A. castellanii*. (**a**) Time-lapse confocal microscopy imaging experiment to monitor the interaction of *A. castellanii* and *V. cholerae*. The amoebae are visible in the transmitted-light channel (labeled Amoebae) and the GFP-producing bacteria in the green channel (labeled *V. cholerae*). The merged signals are shown on the right (labeled Merge). The time p.p.c. is indicated on the left (in h). Amoebae are delineated by solid white lines, whereas the CVs are marked by dashed white lines (valid for all figures). Scale bar: 20 µm. See also Supplementary Movie S1. (**b**) Representative transmission electron micrograph showing undigested bacteria (b) surrounded by a vacuolar membrane (black arrow) compared with cytosolic mitochondria (m) at 3 h p.p.c. (**c**) Undigested *V. cholerae* localize to food vacuoles. Colocalization of GFP-producing bacteria (labeled *V. cholerae*) and Alexa Fluor 647-conjugated dextran (labeled Dextran) within vacuolar compartments of *A. castellanii* at 3 h p.p.c. (amoebal structures are visible in the transmission-light channel; labeled Amoebae). A merged image of the two fluorescent channels is also depicted (labeled Merge). Scale bar: 10 µm. The inset shows a magnification of the white-boxed area in the merged image (scale bar: 2 µm).

leading to the generation of cysts (Bowers and Korn, 1968; Bowers and Korn, 1969; Fouque *et al*., 2012; Siddiqui and Khan, 2012). The major structural changes accompanying encysting trophozoites are (i) the retraction of the pseudopodia; (ii) cell rounding; and (iii) the exocytosis of food vacuole content (Bowers and Korn, 1968; Stewart and Weisman, 1972; Chavez-Munguia *et al*., 2013). During encystment of infected amoebae, however, *V. cholerae* remained within the CV in contrast to the content of the food vacuoles (Figure 4). Moreover, despite encystation, *V. cholerae* grew intracellularly (see below) and lysed the CV, thereby ensuring its release into the cyst's cytosol (Figure 4 and Supplementary Movie S4 and S5). Ultimately, the cysts themselves were lysed, as visualized by the release of fluorescently labeled motile bacteria and influx of dextran through the compromised plasma membrane (Figure 4

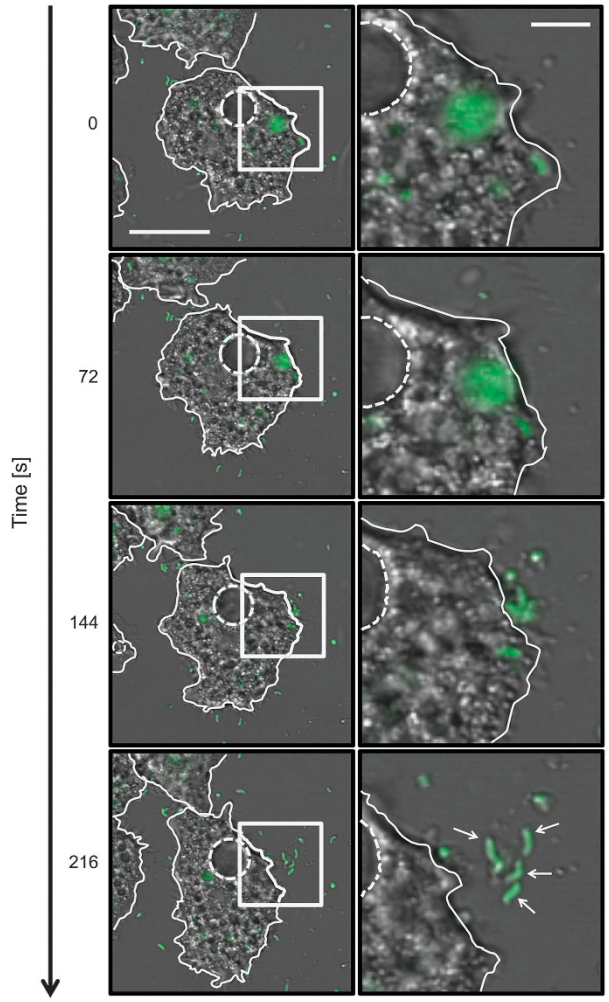


**Figure 2** Release of *V. cholerae* from digestive vacuoles. Time-lapse confocal microscopy image series showing the release of *V. cholerae* from digestive vacuoles. GFP-producing bacteria were incubated with *A. castellanii* for 4.5 h and then monitored over a period of 216 s (relative time shown on the left). Images represent merged transmitted-light (amoebae) and GFP channels (*V. cholerae*). The right row shows magnification of the white-boxed areas highlighted in the left row. The white arrows point to undigested *V. cholerae* released from the food vacuole. Scale bars: 20 and 5 μm for image in the left and right row, respectively. See also Supplementary Movie S2.

and Supplementary Movie S6). Based on these observations, we conclude that lysis of the CV, followed by the lysis of the whole cyst, forms a sequential two-step process allowing *V. cholerae* to return to the environment. Moreover, this behavior defines *V. cholerae* as a pathogen for *A. castellanii* as CV-infected amoebae consistently lysed upon encystment.

*Intracellular proliferation of V. cholerae within the CV*

To test the viability of the *V. cholerae* bacteria within the CV, we used fluorescence recovery after photobleaching. We observed that GFP was resynthesized by the intracellular bacteria, demonstrating their ability for protein synthesis, an indicator of their sustained viability (Supplementary Figure S3). Notably, the recovery kinetics indicated in Supplementary Figure S3 might be an underestimation, as partial killing of bacteria through the iterations of bleaching cannot be excluded.

Moreover, upon observing the accumulation of *V. cholerae* within the *A. castellanii* CV, we wished to determine whether this phenomenon resulted from an accumulation of phagocytosed bacteria (e.g., resulting from a series of vacuolar fusions) or from intracellular growth and proliferation of the pathogen. We therefore infected amoebae with a coculture of *gfp*- or *dsRed*-expressing WT *V. cholerae* strains (at a ratio 1:1; Supplementary Figure S4A). Interestingly, even though dual-colored infected CVs were detectable, single-colored CVs were also observed, indicating that the bacterial population growth resulted from proliferation of one or very few single bacteria (quantified in Table 2). This phenomenon was observed in both the trophozoite and cyst stages (Supplementary Figure S4B).

To further confirm the intracellular growth phenotype, we genetically engineered a growth reporter strain of *V. cholerae* in accordance with previous reports (Bartlett and Gourse, 1994; Sternberg *et al.*, 1999; Nielsen *et al.*, 2010). Such growth reporters are widely used and based on a growth-rate-dependent P1 promoter of ribosomal *rrnB* fused to a reporter gene such as *gfp(ASV)*, which encodes a destabilized version of GFP, which is quickly degraded and suited to study transient gene expression in bacteria (Andersen *et al.*, 1998). It therefore only reports on growing bacteria. This reporter strain allowed us to monitor the growth of cells by observing the accumulation of the fluorescent signal. Indeed, we confirmed the intracellular growth of *V. cholerae* within the CV of both trophozoites and cysts and within the cytosol of cysts (Figure 5). No such fluorescent signal was observable for extracellular bacteria (except for *V. cholerae* cells that recently escaped from burst cysts (Supplementary Figure S4C) owing to the lack of a carbon source in the infection medium, which rendered *V. cholerae* unable to grow extracellularly. These data indicate that *V. cholerae* proliferates within the CV of infected amoebae and within the cytosol of cysts after CV lysis, effectively transforming these compartments into an intracellular replication niche for the pathogen.

*VPS is required for lysis of the CV*

After we had established this intracellular replication niche for *V. cholerae,* we wondered which bacterial factors and/or signal- transduction cascades might be important to establish this host–pathogen interaction. We first focused on QS, which often has a role in virulence regulation in pathogenic bacteria (Rutherford and Bassler, 2012). QS is a cell-to-cell communication system that involves the production and sensing of small molecules, or 'autoinducers'

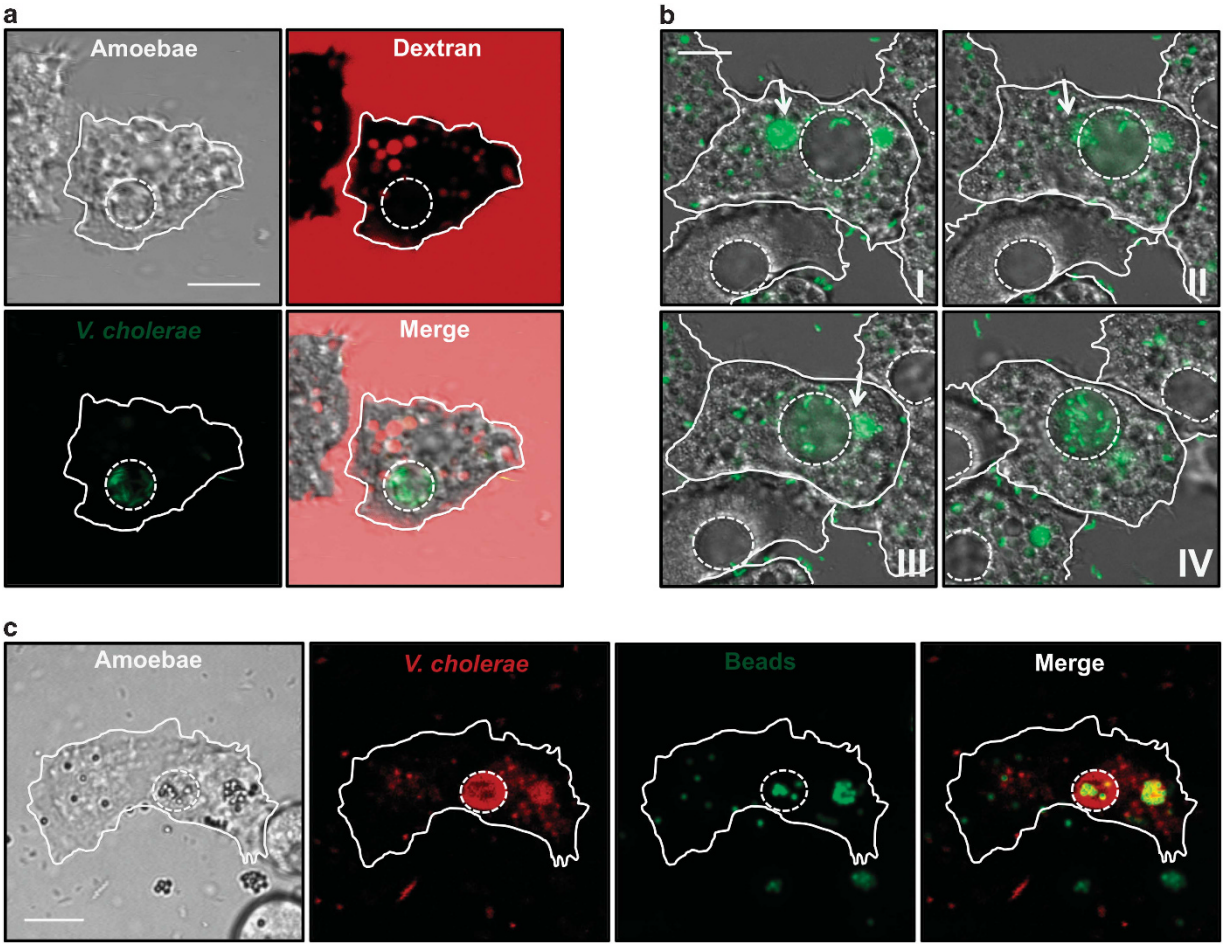


**Figure 3** *V. cholerae* colonizes the CV of *A. castellanii*. (**a**) The amoebae were coincubated with *gfp*-expressing bacteria before confocal laser scanning microscopy (CLSM) imaging. The image composition is as described for Figure 1c, except that the merged image also contains the transmitted-light channel. (**b**) Vacuolar fusion leads to CV colonization. GFP-producing *V. cholerae* (green) were incubated with *A. castellanii* and followed over 6 min starting at 5h07 p.p.c. The relative time is I, 0 s; II, 30 s; III, 60 s; and IV, 360 s. The time series shows the fusion between *V. cholerae*-containing food vacuoles (depicted by the white arrows) and the CV leading to the release of bacteria into the CV. The image composition is as described for Figure 2. See also Supplementary Movie S3. (**c**) Colocalization between *dsRed*-expressing *V. cholerae* (red) and fluorescent beads (green) within the CV. Scale bar for all panels: 10 μm.

within bacterial populations. At high population densities, the concentration of autoinducers is sufficiently elevated to initiate a signaling cascade and to ultimately influence gene expression and bacterial behavior (Platt and Fuqua, 2010). The QS circuit of *V. cholerae* has been extensively studied by Bassler and co-workers. In *V. cholerae,* QS involves the production of the major QS regulator HapR at high cell densities (Ng and Bassler 2009). Previous studies had shown that HapR represses the virulence cascade in *V. cholerae* and decreases the production of extracellular VPS, thereby leading to reduced biofilm formation (Zhu *et al*., 2002; Zhu and Mekalanos, 2003; Hammer and Bassler, 2003; Teschler *et al*., 2015). VPS is primarily composed of glucose and galactose combined with 2-acetamido-2-deoxy-α-L-gulopyranosyluronic acid, glycine and *N*-acetylglucosamine (Yildiz *et al*., 2014; Teschler *et al*., 2015). HapR also acts as a positive regulator of natural competence for transformation and of the bacterium's type VI secretion system (T6SS) (Meibom *et al*., 2005; Zheng *et al*., 2010; Seitz and Blokesch, 2013; Borgeaud *et al*., 2015). We therefore wondered whether *V. cholerae's* QS ability also affected the phenotypes observed in this study. Comparing the dynamics of the intracellular localization of the WT and QS-defective *V. cholerae* strains revealed several altered behaviors such as (i) an overall increase in CV colonization; (ii) a superior CV destruction dynamics; and (iii) enhanced lysis of the amoebal cyst (Figure 6). Indeed, upon careful quantification of these phenotypes, we observed that the HapR-deficient strain showed a statistically significant enhanced CV-related amoebal colonization compared with the WT (3.7% ± 0.6 (s.d.) versus 1.2% ± 0.2 (s.d.); values are averages of three independent experiments and a total of 4200 counted amoebae per strain; $^{**}P = 0.0061$), although CV-colonized trophozoites were rarely detectable (Figure 6b).

Because HapR-deficient strains are known to develop rugose colony morphology and to form enhanced biofilms upon overproduction of VPS (Yildiz and Schoolnik, 1999; Zhu and Mekalanos,

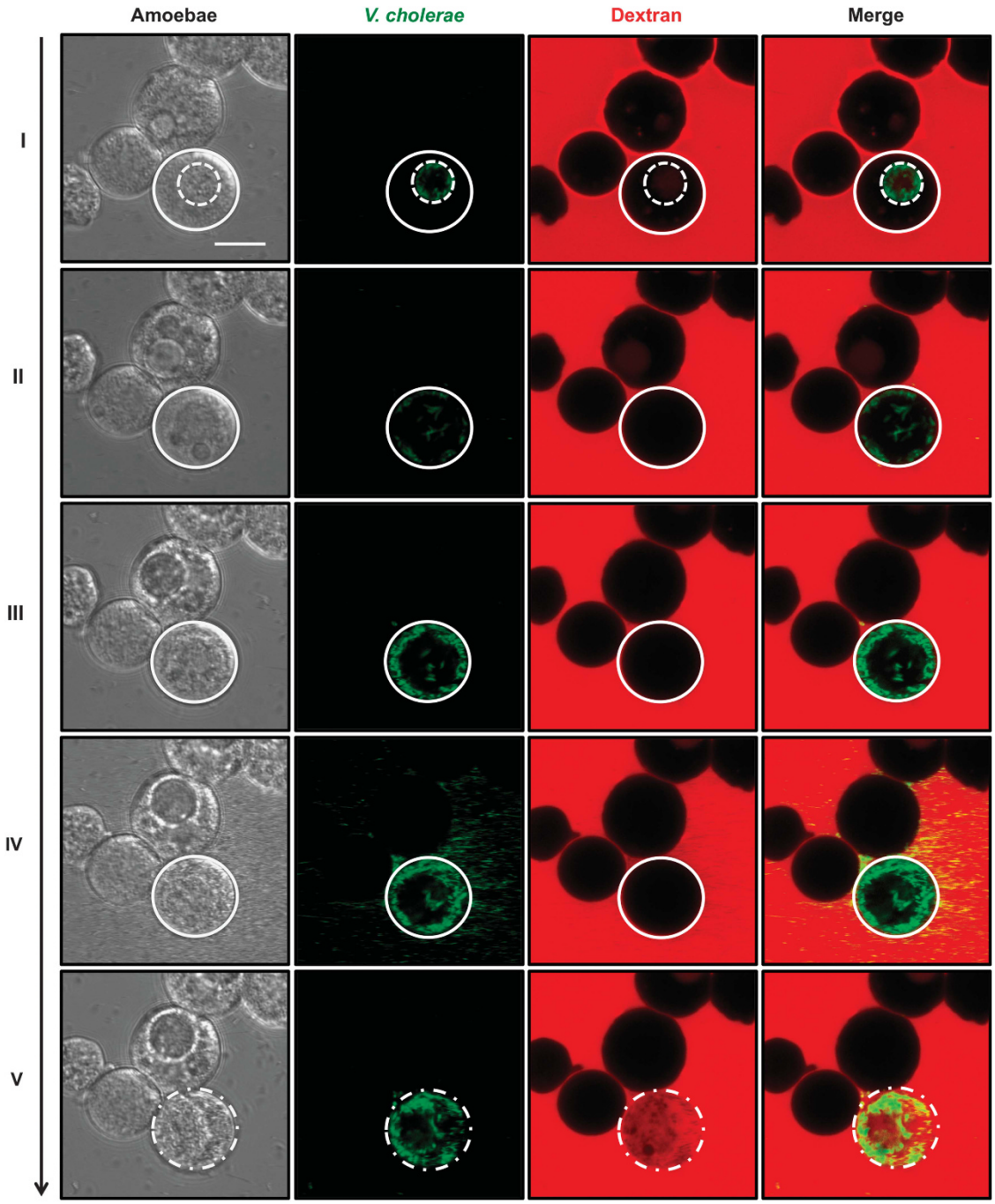


**Figure 4** Cyst lysis occurs after disruption of the *V. cholerae*-colonized CV. Pathogen-containing CVs (I; relative $t = 0$ h, corresponding to 16 h p.p.c.) are lysed within the cyst, which allows the spread of *gfp*-expressing *V. cholerae* into the cyst's cytosol (II; $t = 3.22$ h; Supplementary Movie S4) followed by bacterial proliferation (III; $t = 5.33$ h; Supplementary Movie S5). This leads to the disintegration of the amoebal cell as noted by the escape of *V. cholerae* from the cyst (IV; $t = 5.93$ h; Supplementary Movie S6) and the influx of dextran into the lysed cyst (V; $t = 6.07$ h; Supplementary Movie S6). Scale bar: 10 μm.

2003), we wondered whether the loss of HapR *per se* or the overproduction of VPS contributed to amoebal colonization and CV/cyst lysis. We therefore tested *V. cholerae* strains that lacked the *vpsA* gene, which encodes UDP-*N*-acetylglucosamine 2-epimerase (Fong *et al.*, 2010). This enzyme is required for the production of VPS sugar precursors; thus, *vpsA*-negative (ΔvpsA) strains exhibit reduced VPS production and biofilm formation (Fong *et al.*, 2010). In our amoebal infection model, we noticed that the ΔhapRΔvpsA strain still exhibited a hyper CV colonization phenotype (6.5% ± 1.9 (s.d.) versus 1.2% ± 0.2 (s.d.) for the WT; averages of three independent experiments and a total of 4200 counted amoebae per strain; $^*P = 0.03$) and that ΔvpsA strains were severely impaired in CV lysis,

**Table 2** Mixed color CV colonization assay

| | *Inoculum GFP:dsRed = 1:1* | *Colonized CV* | | |
|---|---|---|---|---|
| | *Mixed colors* | *Mixed colors* | *GFP only* | *dsRed only* |
| Expected (%)[a] | 100% | 100% | 0% | 0% |
| Observed (%)[b] | 100% | 79.7% (±5.5) | 11.7% (±4.1) | 8.6% (±1.6) |
| | Supplementary Figure S4A | | Supplementary Figure S4B | |

[a]Expected percentage values are based on the assumption of repeated vacuolar fusions delivering *V. cholerae* to the CV or single fusion events between one food vacuole containing many bacteria with the CV (e.g., no growth within the CV). [b]Averages are derived from three independent biological experiments (± s.d.).

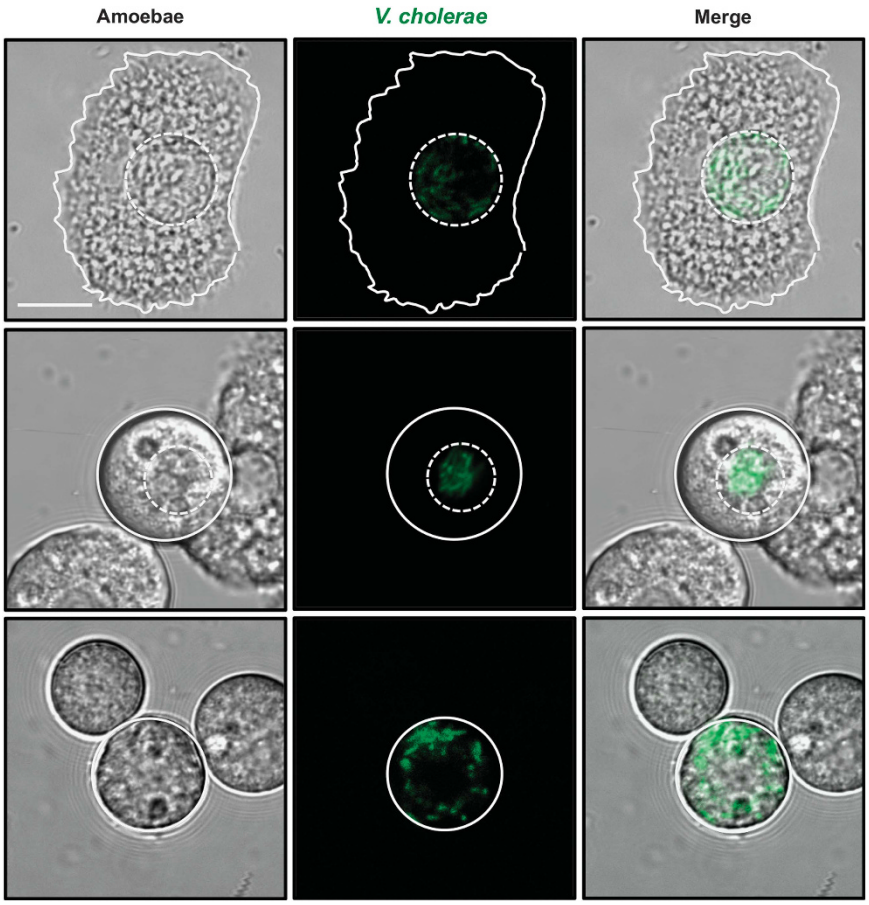


**Figure 5** Evaluation of intracellular growth based on a growth reporter strain. A *V. cholerae* WT strain harboring a chromosomally encoded growth reporter construct was cocultured with *A. castellanii*. Growth of bacteria expressing destabilized GFP was detected in the CVs of trophozoites (upper row), the CVs of cysts (middle row) and the cytosol of cysts (lower row). Scale bar valid for all panels: 10 μm.

regardless of the presence or absence of *hapR* (Figure 6). We therefore conclude that VPS has a critical role in CV lysis. Although the ΔhapR strain often localized to the cytosol of intact or recently lysed cysts, the ΔhapRΔvpsA strain was severely impaired in CV lysis, which was also visible upon inspection of EM images (Figure 6c).

Taken together, these data indicate that QS influences the dynamics of this host–pathogen interaction, that the absence of HapR leads to an increased ability of *V. cholerae* to colonize the CV and that VPS is involved in the CV lysis process.

## Discussion

Cholera is a water-borne disease caused by *V. cholerae*. Understanding the environmental lifestyle of this facultative pathogen is therefore of prime importance as such studies might elucidate the evolutionary development of virulence factors and the mechanisms through which aquatic bacteria transform into human pathogens.

In this study, we examined the interaction of *V. cholerae* with the amoeba *A. castellanii* at the single-cell level. We report a previously

unrecognized interaction mode and therefore propose a novel model of *V. cholerae*'s life cycle in cohabitation with free-living amoebae (Figure 7). The pathogen enters the trophozoite's phago-/endosomal pathway via phagocytosis. However, in contrast to other bacteria (e.g., *E. coli*), a fraction of the *V. cholerae* population resists amoebal digestion. Instead, the bacteria are either exocytosed alive (Figure 2) or enter the CV (Figure 3b). Within this organelle, *V. cholerae* establishes a replication niche, which the pathogen maintains throughout the amoebal encystment process. Bacterial proliferation

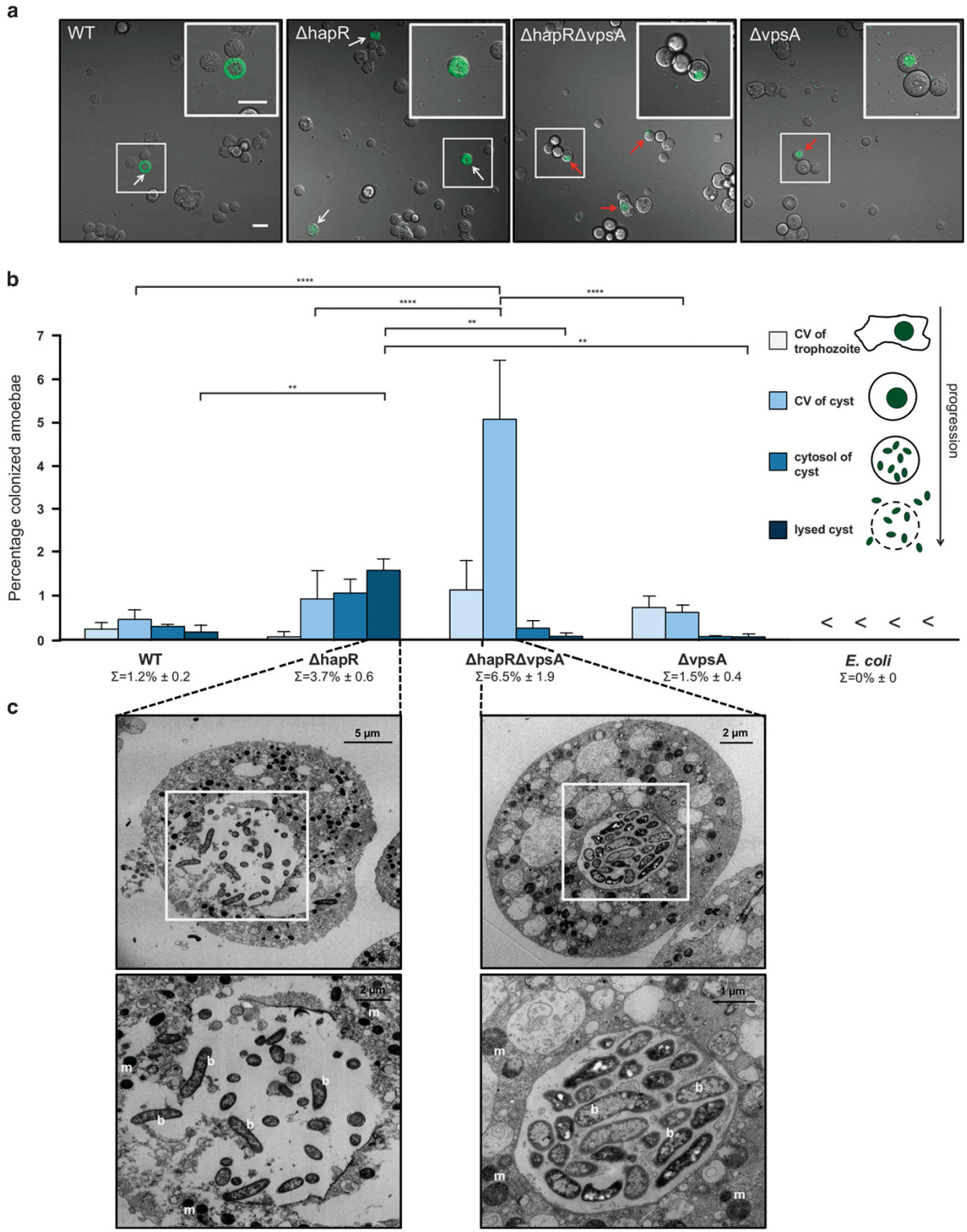

occurs first within the CV; then, *V. cholerae* escapes into the cytosol of the cyst via CV lysis (Figure 4 and Supplementary Movie S4). The CV and the cyst cytosol offer a protective environment for the pathogen's growth (Figure 4 and Supplementary Movie S5) until a cyst-lysis event releases the bacteria back into the environment (Figure 4 and Supplementary Movie S6).

At this stage, it is unclear whether the encystment, CV destruction and/or amoebal lysis are actively induced by the pathogen or whether colonization of the CV hinders the normal osmoregulatory function of the organelle, which ultimately results in passive CV and cyst lysis. However, we provide evidence that the bacterial VPS is of prime importance for the lysis of the CV (Figure 6). We therefore hypothesize

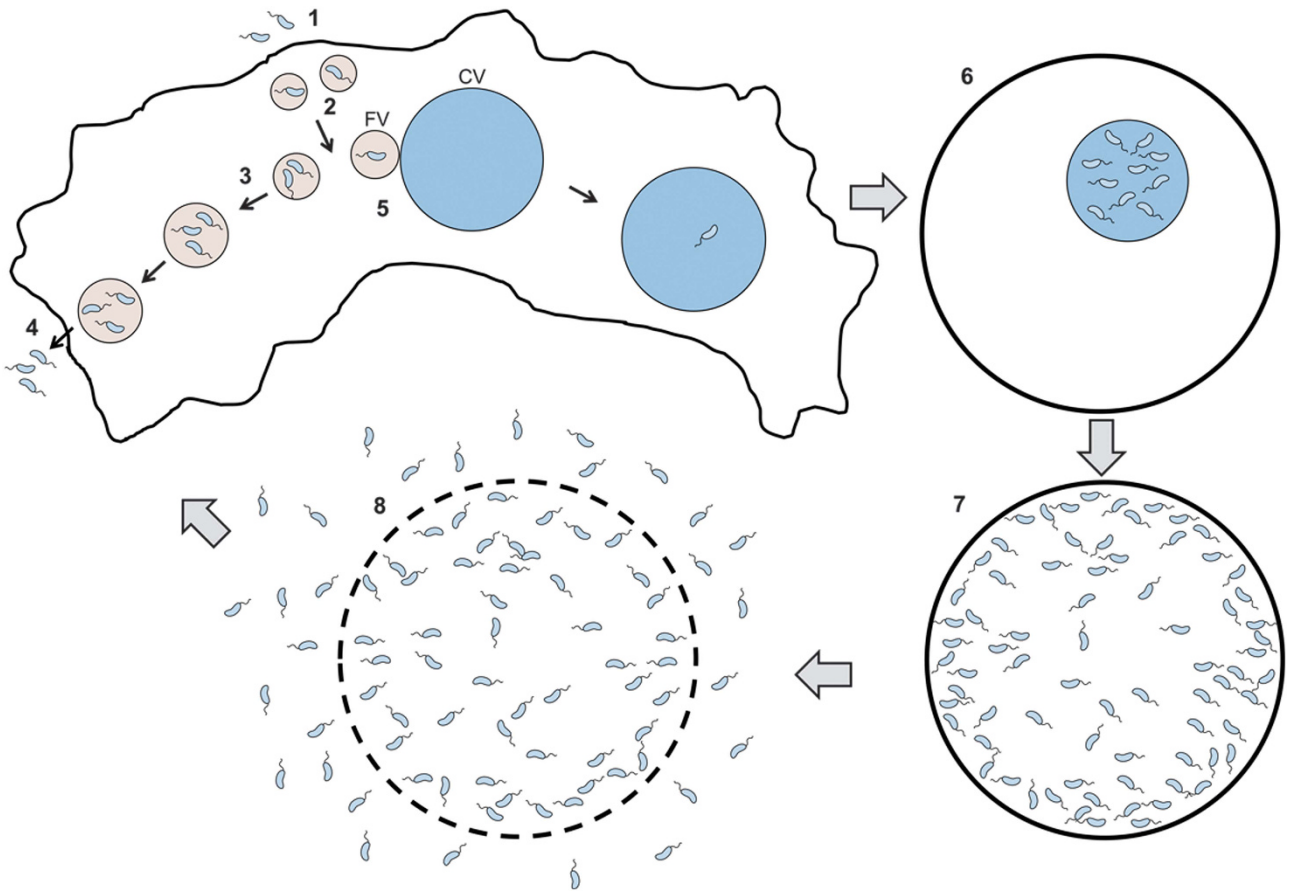


**Figure 7** Scheme summarizing the interaction between *V. cholerae* and *A. castellanii*. Upon phagocytosis of free *V. cholerae* cells (1) by amoebal trophozoites, the bacteria are contained in endosomal vacuoles (2). Fusion of endosomal vacuoles leads to the generation of large vacuoles (3). The content of small and large vacuoles is frequently emptied by *A. castellanii* (4), thereby releasing live bacteria back into the environment. At times endosomal vacuoles can also shuffle *V. cholerae* cells into the CV (5), which allows the bacteria to establish a replication niche. When amoebae containing such colonized CVs undergo encystment, the digestive vacuoles are emptied but *V. cholerae* remains within the cyst's CV (6). *V. cholerae* proliferates in this protective environment, ultimately leading to CV lysis (7). This process is dependent on VPS. Finally, weakening of the cyst cell wall occurs (8), leading to the release of the intracellular proliferating *V. cholerae* cells into the extracellular environment.

**Figure 6** The VPS contributes to CV lysis. (**a**) *V. cholerae* strains lacking VPS are severely impaired in amoebal CV lysis. Confocal imaging of amoebal cysts formed in the presence of *V. cholerae* WT strain (WT) or mutant *V. cholerae* strains lacking *hapR* (ΔhapR), *vpsA* (ΔvpsA) or *hapR* and *vpsA* (ΔhapRΔvpsA). White arrows depict *V. cholerae* within the cytosol of the cysts after CV lysis and red arrows indicate colonized but intact CVs. Shown are merged images of the transmitted light and the GFP channels taken at 20 h p.p.c. The insets show magnifications of the boxed regions. Scale bars: 20 μm. (**b**) Quantification of specific events during amoebal colonization. *A. castellanii* cells harboring *V. cholerae* inside the CV of the trophozoite, the CV of the cyst and within the cytosol of the cyst before and after cyst lysis were counted. Values represent averages from three independent experiments (4200 total amoebae counted for each strain). <, below the detection limit of 0.02%. Statistically significant differences are indicated (****$P<0.0001$; **$P<0.01$). Σ indicates the total percentage of colonized CVs per *V. cholerae* strain (± s.d.). (**c**) Representative transmission electron micrographs showing colonized compartments of *A. castellanii*. *V. cholerae* strains ΔhapR and ΔhapRΔvpsA were cocultured with *A. castellanii* for 20 h before infected cysts were visualized by electron microscopy. The lower images are magnifications of the boxed regions in the upper images. b, bacteria; m, mitochondria. *V. cholerae* strains used for all panels were producing fluorescent proteins.

that the extracellular polysaccharide might hamper CV contraction-dependent osmoregulation of *A. castellanii*, potentially through an agglutination effect, which leads to lysis of the organelle and ultimately the whole amoeba. Such VPS-mediated agglutination is consistent with an impaired intracellular motility that was observed for the VPS-overproducing HapR-deficient strain (compare the even distribution of ΔhapR bacteria to the motility-driven circular localization of WT in the cytosol of the cysts; Figure 6a and Supplementary Movie S5 and S6). This study therefore suggests that selective pressure exerted on bacterial pathogens in their natural environments can lead to unique pathogenic traits such as the production of polysaccharide. Indeed, the majority of *V. cholerae* cells that lacked VPS were unable to exit their amoebal host (Figure 6), and this characteristic would therefore be counter-selected in nature. Intriguingly, the production of VPS is also important for intestinal colonization, as VPS-mutant strains of *V. cholerae* show a colonization defect in the infant mouse model compared with their WT parental strain (Fong *et al*., 2010).

Previous studies have suggested that survival of *V. cholerae* O1 strains (classical and El Tor) and *A. castellanii* is enhanced in cocultivation experiments performed in rich peptone yeast glucose medium (ATCC medium 712) (Abd *et al*., 2007). Moreover, the authors reported intracellular *V. cholerae* growth for up to 14 days (Abd *et al*., 2007), which is not consistent with the forced release of the bacteria that we observed in this study after intracellular proliferation (Figure 4 and Supplementary Movie S4–S6). Notably, when we repeated the experiments described by Abd *et al*., 2007 we observed massive extracellular proliferation of *V. cholerae* within the rich medium, which fully sustained bacterial growth. Thus, in agreement with the high numbers of extracellular *V. cholerae* detected by Abd *et al*. (2007, 2011) in the coculture experiments (allegedly up to $2 \times 10^{11}$ CFU ml$^{-1}$ as stated in Abd *et al.* (2007) and Abd *et al.* (2011)), it is possible that the authors scored recent phagocytosis events as 'intracellularly growing bacteria'. Indeed, extracellular bacteria were not killed throughout the experiment but solely at the time of sampling (Abd *et al*., 2007). To avoid such extracellular proliferation of the pathogen in the current study, we used an infection medium that does not sustain bacterial growth. Moreover, in addition to scoring CFUs, we directly imaged the intracellular behavior and growth of *V. cholerae*. Using these methods, combined with electron microscopy imaging, we provide evidence for the absence of free *V. cholerae* within the cytosol of trophozoites, contrary to previous claims (Abd *et al*., 2005, 2007, 2011), even though mitochondria were easily detected (Figure 1b) (which can be misled for cross-sectioned bacteria if the mitochondrial cristae structures are not well preserved or overstained). Instead, we primarily uncovered *V. cholerae* in small and large food vacuoles as part of the phago-/endosomal pathway and frequently observed exocytosis of undigested bacteria (Figure 2). Most importantly, we consistently detected a small percentage of the amoebal population with proliferating *V. cholerae* cells contained within their CV (Figures 3–5). To our knowledge, this is the first report showing active colonization of the CV by a pathogen through vacuolar fusion, followed by proliferation, encystment of the host and CV lysis. Although, a previous study showed that rare CV colonization by *Salmonella* occurred when *A. polyphaga* encountered a high (packing) density of surrounding bacteria (specifically when amoebae were spotted onto bacterial lawns formed on agar plates and observed after 2–4 days p.p.c.) (Gaze *et al*., 2003). Gaze *et al*. (2003) hypothesized that the *Salmonella* entered the CV via reflux through the pore during contraction-dependent fluid discharge and concluded that 'the fate of the amoebae and bacteria following this interaction is unknown'. Based on the data presented for *V. cholerae* in this study, we conclude that the CV represents a new replication niche in which the bacterium is protected against external stresses (e.g., phages, competing bacteria) and intracellular stresses (e.g., vacuole acidification, anti-microbial compounds). The proposed bacterial strategy avoids destruction of the entire predator population, which can be favorable for environmental purposes and would result in a long-term equilibrium between amoebae and *V. cholerae*. A similar scenario occurs for cholera as a human disease, in which the majority of infected persons do not show symptoms (WHO, 2011). Instead, only a small fraction of infected people suffer from severe diarrhea, which is accompanied by massive bacterial proliferation and the release of the pathogen back into the environment.

## Conflict of Interest

The authors declare no conflict of interest.

## Acknowledgements

We thank Sandrine Borgeaud for technical assistance and Gilbert Greub and Sebastien Aeby for providing us with the *Acanthamoeba castellanii* strain and for valuable methodological advice. We are indebted to Graham Knott from the Bioelectron Microscopy Core Facility for discussions on the project. We also acknowledge Thierry Soldati for advice and helpful comments on the manuscript and John McKinney, Pierre Cosson, Matthieu Delincé, and Ana T. López-Jiménez for fruitful discussions. This work was supported by grants from the European Research Council (309064-VIR4ENV) and the Swiss National Science Foundation (31003A_143356) to MB.

## References

Abd H, Saeed A, Weintraub A, Nair GB, Sandström G. (2007). *Vibrio cholerae* O1 strains are facultative intracellular bacteria, able to survive and multiply symbiotically inside the aquatic free-living amoeba *Acanthamoeba castellanii*. *FEMS Microbiol Ecol* **60**: 33–39.

Abd H, Shanan S, Saeed A, Sandström G. (2011). Survival of *Vibrio cholerae* inside *Acanthamoeba* and detection of both microorganisms from natural water samples may point out the amoeba as a protozoal host for *V. cholerae*. *Bacteriol Parasitol* S1-003; doi:10.4172/2155-9597.S1-003.

Abd H, Weintraub A, Sandström G. (2005). Intracellular survival and replication of *Vibrio cholerae* O139 in aquatic free-living amoebae. *Environ Microbiol* **7**: 1003–1008.

Allen RD. (2000). The contractile vacuole and its membrane dynamics. *BioEssays* **22**: 1035–1042.

Andersen JB, Sternberg C, Poulsen LK, Bjorn SP, Givskov M, Molin S. (1998). New unstable variants of green fluorescent protein for studies of transient gene expression in bacteria. *Appl Environ Microbiol* **64**: 2240–2246.

Aubry L, Klein G, Martiel JL, Satre M. (1993). Kinetics of endosomal pH evolution in *Dictyostelium discoideum* amoebae. Study by fluorescence spectroscopy. *J Cell Sci* **105**: 861–866.

Bao Y, Lies DP, Fu H, Roberts GP. (1991). An improved Tn*7*-based system for the single-copy insertion of cloned genes into chromosomes of Gram-negative bacteria. *Gene* **109**: 167–168.

Bartlett MS, Gourse RL. (1994). Growth rate-dependent control of the *rrnB* P1 core promoter in *Escherichia coli*. *J Bacteriol* **176**: 5560–5564.

Blokesch M. (2012a). TransFLP—a method to genetically modify *V. cholerae* based on natural transformation and FLP-recombination. *J Vis Exp* **68**: e3761.

Blokesch M. (2012b). Chitin colonization, chitin degradation and chitin-induced natural competence of Vibrio cholerae are subject to catabolite repression. *Environ Microbiol* **14**: 1898–1912.

Borgeaud S, Blokesch M. (2013). Overexpression of the *tcp* gene cluster using the T7 RNA polymerase/promoter system and natural transformation-mediated genetic engineering of *Vibrio cholerae*. *PLoS One* **8**: e53952.

Borgeaud S, Metzger LC, Scrignari T, Blokesch M. (2015). The type VI secretion system of *Vibrio cholerae* fosters horizontal gene transfer. *Science* **347**: 63–67.

Bowers B, Korn ED. (1968). The fine structure of *Acanthamoeba castellanii*. I. The trophozoite. *J Cell Biol* **39**: 95–111.

Bowers B, Korn ED. (1969). The fine structure of *Acanthamoeba castellanii* (Neff strain). II. Encystment. *J Cell Biol* **41**: 786–805.

Chavez-Munguia B, Salazar-Villatoro L, Lagunes-Guillen A, Omana-Molina M, Espinosa-Cantellano M, Martinez-Palomo A. (2013). *Acanthamoeba castellanii* cysts: new ultrastructural findings. *Parasitol Res* **112**: 1125–1130.

Colwell RR. (1996). Global climate and infectious disease: the cholera paradigm. *Science* **274**: 2025–2031.

De Souza Silva O, Blokesch M. (2010). Genetic manipulation of *Vibrio cholerae* by combining natural transformation with FLP recombination. *Plasmid* **64**: 186–195.

Doberstein SK, Baines IC, Wiegand G, Korn ED, Pollard TD. (1993). Inhibition of contractile vacuole function *in vivo* by antibodies against myosin-I. *Nature* **365**: 841–843.

Fong JC, Syed KA, Klose KE, Yildiz FH. (2010). Role of *Vibrio* polysaccharide (*vps*) genes in VPS production, biofilm formation and *Vibrio cholerae* pathogenesis. *Microbiology* **156**: 2757–2769.

Fouque E, Trouilhe MC, Thomas V, Hartemann P, Rodier MH, Hechard Y. (2012). Cellular, biochemical, and molecular changes during encystment of free-living amoebae. *Eukaryot Cell* **11**: 382–387.

Gaze WH, Burroughs N, Gallagher MP, Wellington EM. (2003). Interactions between *Salmonella typhimurium* and *Acanthamoeba polyphaga*, and observation of a new mode of intracellular growth within contractile vacuoles. *Microb Ecol* **46**: 358–369.

Gilbert JA, Steele JA, Caporaso JG, Steinbruck L, Reeder J, Temperton B *et al.* (2012). Defining seasonal marine microbial community dynamics. *ISME J* **6**: 298–308.

Greub G, Raoult D. (2004). Microorganisms resistant to free-living amoebae. *Clin Microbiol Rev* **17**: 413–433.

Hammer BK, Bassler BL. (2003). Quorum sensing controls biofilm formation in *Vibrio cholerae*. *Mol Microbiol* **50**: 101–104.

Hoffmann C, Harrison CF, Hilbi H. (2014). The natural alternative: protozoa as cellular models for *Legionella* infection. *Cell Microbiol* **16**: 15–26.

Khan NA. (2006). *Acanthamoeba*: biology and increasing importance in human health. *FEMS Microbiol Rev* **30**: 564–595.

Khan NA. (2015). *Acanthamoeba—Biology and Pathogenesis*, 2nd edn. Caister Academic Press: Norfolk, UK.

Martinez AJ, Visvesvara GS. (1997). Free-living, amphizoic and opportunistic amebas. *Brain Pathol* **7**: 583–598.

Marvig RL, Blokesch M. (2010). Natural transformation of *Vibrio cholerae* as a tool-optimizing the procedure. *BMC Microbiol* **10**: 155.

Matz C, Kjelleberg S. (2005). Off the hook—how bacteria survive protozoan grazing. *Trends Microbiol* **13**: 302–307.

Matz C, McDougald D, Moreno AM, Yung PY, Yildiz FH, Kjelleberg S. (2005). Biofilm formation and phenotypic variation enhance predation-driven persistence of *Vibrio cholerae*. *Proc Natl Acad Sci USA* **102**: 16819–16824.

Meibom KL, Blokesch M, Dolganov NA, Wu C-Y, Schoolnik GK. (2005). Chitin induces natural competence in *Vibrio cholerae*. *Science* **310**: 1824–1827.

Morens DM, Folkers GK, Fauci AS. (2004). The challenge of emerging and re-emerging infectious diseases. *Nature* **430**: 242–249.

Müller J, Miller MC, Nielsen AT, Schoolnik GK, Spormann AM. (2007). *vpsA*- and *luxO*-independent biofilms of *Vibrio cholerae*. *FEMS Microbiol Lett* **275**: 199–206.

Nelson EJ, Chowdhury A, Harris JB, Begum YA, Chowdhury F, Khan AI *et al.* (2007). Complexity of rice-water stool from patients with *Vibrio cholerae* plays a role in the transmission of infectious diarrhea. *Proc Natl Acad Sci USA* **104**: 19091–19096.

Ng WL, Bassler BL. (2009). Bacterial quorum-sensing network architectures. *Annu Rev Genet* **43**: 197–222.

Nielsen AT, Dolganov NA, Rasmussen T, Otto G, Miller MC, Felt SA *et al.* (2010). A bistable switch and anatomical

site control *Vibrio cholerae* virulence gene expression in the intestine. *PLoS Pathogen* **6**: e1001102.
Pernthaler J. (2005). Predation on prokaryotes in the water column and its ecological implications. *Nat Rev Microbiol* **3**: 537–546.
Platt TG, Fuqua C. (2010). What's in a name? The semantics of quorum sensing. *Trends Microbiol* **18**: 383–387.
Pukatzki S, Ma AT, Sturtevant D, Krastins B, Sarracino D, Nelson WC *et al.* (2006). Identification of a conserved bacterial protein secretion system in *Vibrio cholerae* using the *Dictyostelium* host model system. *Proc Natl Acad Sci USA* **103**: 1528–1533.
Rutherford ST, Bassler BL. (2012). Bacterial quorum sensing: its role in virulence and possibilities for its control. *Cold Spring Harbor Perspect Med* **2**: a012427.
Sandström G, Saeed A, Abd H. (2010). *Acanthamoeba polyphaga* is a possible host for *Vibrio cholerae* in aquatic environments. *Exp Parasitol* **126**: 65–68.
Seitz P, Blokesch M. (2013). Cues and regulatory pathways involved in natural competence and transformation in pathogenic and environmental Gram-negative bacteria. *FEMS Microbiol Rev* **37**: 336–363.
Shanan S, Abd H, Hedenström I, Saeed A, Sandström G. (2011). Detection of *Vibrio cholerae* and *Acanthamoeba* species from same natural water samples collected from different cholera endemic areas in Sudan. *BMC Res Notes* **4**: 109.
Siddiqui R, Khan NA. (2012). Biology and pathogenesis of *Acanthamoeba*. *Parasites Vectors* **5**: 6.
Snelling WJ, Moore JE, McKenna JP, Lecky DM, Dooley JS. (2006). Bacterial-protozoa interactions; an update on the role these phenomena play towards human illness. *Microbes Infect* **8**: 578–587.
Solomon JM, Isberg RR. (2000). Growth of *Legionella pneumophila* in *Dictyostelium discoideum*: a novel system for genetic analysis of host-pathogen interactions. *Trends Microbiol* **8**: 478–480.
Sternberg C, Christensen BB, Johansen T, Toftgaard Nielsen A, Andersen JB, Givskov M *et al.* (1999). Distribution of bacterial growth activity in flow-chamber biofilms. *Appl Environ Microbiol* **65**: 4108–4117.
Stewart JR, Weisman RA. (1972). Exocytosis of latex beads during the encystment of *Acanthamoeba*. *J Cell Biol* **52**: 117–130.
Sun S, Kjelleberg S, McDougald D. (2013). Relative contributions of *Vibrio* polysaccharide and quorum sensing to the resistance of *Vibrio cholerae* to predation by heterotrophic protists. *PLoS One* **8**: e56338.
Swanson MS, Hammer BK. (2000). *Legionella pneumophila* pathogesesis: a fateful journey from amoebae to macrophages. *Annu Rev Microbiol* **54**: 567–613.
Takemura AF, Chien DM, Polz MF. (2014). Associations and dynamics of Vibrionaceae in the environment, from the genus to the population level. *Front Microbiol* **5**: 38.
Teschler JK, Zamorano-Sanchez D, Utada AS, Warner CJ, Wong GC, Linington RG *et al.* (2015). Living in the matrix: assembly and control of *Vibrio cholerae* biofilms. *Nat Rev Microbiol* **13**: 255–268.
Thom S, Warhurst D, Drasar BS. (1992). Association of *Vibrio cholerae* with fresh water amoebae. *J Med Microbiol* **36**: 303–306.
WHO (2011). *Fact sheet No.107*. WHO: Geneva, Switzerland.
Yildiz F, Fong J, Sadovskaya I, Grard T, Vinogradov E. (2014). Structural characterization of the extracellular polysaccharide from *Vibrio cholerae O1* El-Tor. *PLoS One* **9**: e86751.
Yildiz FH, Schoolnik GK. (1998). Role of *rpoS* in stress survival and virulence of *Vibrio cholerae*. *J Bacteriol* **180**: 773–784.
Yildiz FH, Schoolnik GK. (1999). *Vibrio cholerae* O1 El Tor: identification of a gene cluster required for the rugose colony type, exopolysaccharide production, chlorine resistance, and biofilm formation. *Proc Natl Acad Sci USA* **96**: 4028–4033.
Yooseph S, Nealson KH, Rusch DB, McCrow JP, Dupont CL, Kim M *et al.* (2010). Genomic and functional adaptation in surface ocean planktonic prokaryotes. *Nature* **468**: 60–66.
Zheng J, Shin OS, Cameron DE, Mekalanos JJ. (2010). Quorum sensing and a global regulator TsrA control expression of type VI secretion and virulence in *Vibrio cholerae*. *Proc Natl Acad Sci USA* **107**: 21128–21133.
Zhu J, Mekalanos JJ. (2003). Quorum sensing-dependent biofilms enhance colonization in *Vibrio cholerae*. *Dev Cell* **5**: 647–656.
Zhu J, Miller MB, Vance RE, Dziejman M, Bassler BL, Mekalanos JJ. (2002). Quorum-sensing regulators control virulence gene expression in *Vibrio cholerae*. *Proc Natl Acad Sci USA* **99**: 3129–3134.



Supplementary Information accompanies this paper on The ISME Journal website (http://www.nature.com/ismej)